Optimization of high-definition video coding and hybrid fiber-wireless transmission in the 60 GHz band

Alexander Lebedev,[1,*] Tien Thang Pham,[1] Marta Beltrán,[2] Xianbin Yu,[1] Anna Ukhanova,[1] Roberto Llorente,[2] Idelfonso Tafur Monroy,[1] and Søren Forchhammer[1]

[1]*DTU Fotonik, Department of Photonics Engineering, Technical University of Denmark, 2800 Kgs. Lyngby, Denmark*
[2]*Valencia Nanophotonics Technology Center, Universidad Politécnica de Valencia, Camino de Vera s/n, 46022 Valencia, Spain*
[*]alele@fotonik.dtu.dk

Abstract: The paper addresses the problem of distribution of high-definition video over fiber-wireless networks. The physical layer architecture with the low complexity envelope detection solution is investigated. We present both experimental studies and simulation of high quality high-definition compressed video transmission over 60 GHz fiber-wireless link. Using advanced video coding we satisfy low complexity and low delay constraints, meanwhile preserving the superb video quality after significantly extended wireless distance.

References and links

1. M. Beltrán, J. B. Jensen, X. Yu, R. Llorente, and I. T. Monroy, "Experimental performance comparison of 60 GHz DCM OFDM and impulse BPSK ultra-wideband with combined optical fibre and wireless transmission," in ECOC, 1465–1467 (2010).
2. Z. Jia, H.-C. Chien, Y.-T. Hsueh, A. Chowdhury, J. Yu, and G.-K. Chang, "Wireless HD services over optical access systems: Transmission, networking, and demonstration," in OFC, 1–5 (2009).
3. M. Weiß, "60 GHz photonic millimeter-wave communication systems," thesis (2010).
4. A. Belogolovy, E. Belyaev, A. Sergeev, and A. Turlikov, "Video compression for wireless transmission: reducing the power consumption of the WPAN hi-speed systems," NEW2AN/ruSMART 2009, LNCS 5764, 313–322 (2009).
5. http://iphome.hhi.de/suehring/tml/.
6. T. Stockhammer, M. M. Hannuksela, and T. Wiegand, "H.264/AVC in wireless environments," IEEE Trans.Circuits Syst. Video Technol. **13**(7), 657–673 (2003).
7. I. E. Richardson, *The H.264 Advanced Video Compression Standard* (Wiley, 2010).
8. http://www.vpiphotonics.com/.
9. S.-K. Yong, *60 GHz Technology for Gbps WLAN and WPAN: From Theory to Practice* (Wiley, 2011), Chap. 2.
10. S. K. Yong and C.-C. Chong, "An overview of multigigabit wireless through millimeter wave technology: potentials and technical challenges," EURASIP J. Wireless Commun. Netw. **2007**(1), 078907 (2007).
11. K.-C. Huang and D. J. Edwards, *Millimetre Wave Antennas for Gigabit Wireless Communications: A Practical Guide to Design and Analysis in a System Context* (Wiley, 2008).

1. Introduction

The motivations for this work are three-fold. First, the unprecedented frequency range around 60 GHz (from 4 to 9 GHz within 57-66 GHz) has been regulated for unlicensed use in a number of countries around the world. Second motivation is the introduction of high quality video services such as high-definition (HD) video conferencing and distributed video gaming. These services define both the demand for increased data rates in the access networks and need for optimization of video compression schemes. Third, efficient convergence of wired and wireless technologies is required to enable the concept of "anytime anywhere" wireless

connectivity. Radio-over-fiber (RoF) is considered a promising example of such integration for optical networks [1].

Previous research in the area of 60 GHz RoF video transmission suggests the use of uncompressed video [2,3]. The main drawback of this approach is reduced flexibility in terms of bitrate: bitrates are fixed depending on resolution, number of bits per pixel, and frame rate of the video sequence. This therefore results in extremely complex adaptation of the HD video system to significant signal-to-noise ratio (SNR) drops caused by either severe shadowing in non-line-of-sight (NLOS) case or extremely high attenuation – problems that are typical for 60 GHz systems.

Source coding (compression) gives us desirable flexibility of bitrate but at the expense of introducing delay and increase of power consumption. However, there is a trade-off between the power needed to radiate larger bandwidth for uncompressed video and the power consumed for the computations of an encoder and a decoder for compressed video transmission. According to [4], low complexity compression can, in fact, bring about reduction in power consumption for a 60 GHz wireless video transmission system compared to the uncompressed case, while at the same time keeping delay under the acceptable limit.

In this work we explore the notion of joint optimization of physical layer parameters of a RoF link (power levels, distance) and the codec parameters (quantization, error-resilience tools) based on peak signal-to-noise ratio (PSNR) as an objective video quality metric. We experimentally demonstrate, first time to our knowledge, the combined optical access and wireless transmission of compressed HD video in the 60 GHz band employing simple envelope detection technique.

2. Experimental setup

The experimental setup of the 60 GHz optical-wireless RoF system is shown in Fig. 1. The binary sequence corresponding to compressed video file was uploaded in an arbitrary waveform generator (AWG). The non-return-to-zero (NRZ) electrical signal on the output of the AWG directly modulated a 1550 nm laser. After the baseband data modulation, frequency up-conversion to the 60 GHz band was performed by driving a Mach-Zehnder modulator (MZM) biased at the minimum transmission point with a 30 GHz sinusoidal signal. A polarization controller (PC) was used before the MZM to minimize its polarization-dependant losses. After the MZM, two sidebands with a frequency spacing of $2f_{LO}$ were generated according to the double sideband-suppressed carrier (DSB-SC) intensity modulation scheme (see Fig. 2). Optical carrier suppression of approximately 13.6 dB is achieved limited by the MZM extinction ratio. The generated sidebands have the same optical power and the locked phase. Subsequently, an Erbium doped fiber amplifier (EDFA) is employed to compensate the losses, and an optical band pass filter (OBPF) is used afterwards to mitigate the amplified spontaneous emission (ASE) noise produced by the EDFA. Then the signal is launched into a 20 km span of non-zero dispersion shifted fiber (NZDSF). We employ the NZDSF in order to minimize dispersion induced impairments. A variable optical attenuator (VOA) is employed to control the optical power impinging the photodiode (PD) in order to evaluate BER performance of the system as a function of the received optical power.
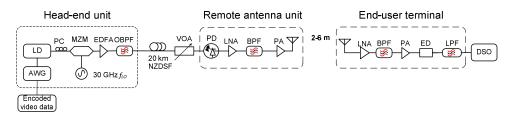
Fig. 1. Experimental 60 GHz optical-wireless RoF system with envelope detection, LD-laser diode, PC-polarization controller, MZM-Mach-Zehnder modulator, LO-local oscillator, EDFA-Erbium doped fiber amplifier, OBPF-optical band pass flilter, PD-photodiode, LNA-low noise amplifier, PA-power amplifier, BPF-band pass filter, ED- envelope detector, LPF-low pass filter, DSO-digital sampling oscilloscope.

After photodetection the 60 GHz signal was amplified (gain of amplifiers – 16 dB and 28.7 dB) and filtered (58.1-61.9 GHz) before feeding it to an antenna for up to 6 meters of wireless transmission. After receiving the signal with an antenna and following filtering (58.1-61.9 GHz) and amplification (gain of amplifiers – 16 dB and 28.7 dB) envelope detection was employed for down-conversion. The detected envelope is low-pass filtered and digitized by a digital sampling oscilloscope (DSO). Both the transmitting and receiving antennas used throughout the experiment are commercially available horn antennas with 20 dBi gain and 12° beam width. Bitrates that were transmitted over the fiber are low compared to similar research setups. This explains a good performance to a certain extent, but we emphasize that reduction of bitrate does not lead to a significant video quality deterioration.
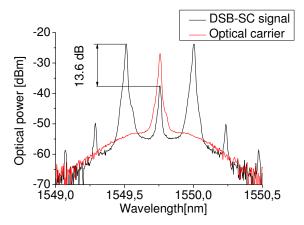

Fig. 2. Optical spectra on the input of the PD.

The encoding was performed using the Joint Model (JM) 17.0 reference software implementation of the H.264/Advanced Video Codec (AVC) [5]. It is a realistic scenario since H.264/AVC is one of the latest industrial video coding standards covering a wide range of applications, including, coding for transmission over wireless links and HDTV coding [6]. An Intra coding mode only and a frame slicing mechanism were employed to achieve the low delay requirement. Both mechanisms are improving the error-resilience as well [7]. Slicing was performed with the use of flexible macroblock ordering (FMO).

H.264 is not capable of coping with single-bit errors: its mechanisms of error-resilience on the encoding side and error concealment on the decoding side are adjusted to cope with packet loss when the packets affected by the errors are discarded such as usually occurs in networks. Packet error rate (PER) depends on the bit error rate (BER) and the size of the packet; in general, the noisier the transmission the shorter the length of the packet is desirable. Initially in the experiment we used the packet size equal to 2500 bytes, each packet containing a slice of the frame; afterwards we have been using packets of length of 3000 and 3500 bytes for

simulation. The uncompressed HD test video sequence 'blue sky' was used for encoding and transmission. The sequence was originally shot in 4:2:0 format 8 bits per color 1920 × 1080 pixels. However, in order to model the most bitrate demanding case upsampling to 4:4:4 format was performed (uncompressed bitrate – 3 Gbps for the frame rate of 60 frames per second).

We use PSNR as an objective quality metric for video, which is defined as:

$$MSE = \frac{1}{N} \sum_{i=1}^{N} (x_i - y_i)^2,$$ (1)

$$PSNR = 10 \log_{10} (\frac{L^2}{MSE}),$$ (2)

where MSE stands for mean squared error, N is the number of pixels in the image or video signal, and x_i and y_i are the i-th pixel values in the original and the distorted signals, respectively. L is the dynamic range of the pixel values. For an 8 bits/pixel signal, L is equal to 255. PSNR is evaluated for the luminance component of the transmitted video signal.

3. Composite fiber-wireless channel modeling for 60 GHz band

The difficulty of the modeling arises from the fact that we need to account for both the impairments induced by the wireless and the fiber-optic channels. We performed the modeling of the fiber-optic channel with VPI software [8]. The wireless channel model was implemented in Matlab and combined with VPI channel model afterwards. We combine below the description of the channel model with the excerpts from experimental measurements that allow us to simplify the model.

Noise processes in the optical part of the setup (such as amplified spontaneous emission (ASE) noise, Johnson noise, shot noise at the photodiode), attenuation and dispersion in the fiber are simulated in VPI software. We set the numerical values for these parameters according to the specifications of equipment we used in the experimental setup.

We performed the modeling of the wireless channel according to the physical parameters of the devices that have been used in the scheme and references on theoretical parameters taken from [9–11].

The path loss (attenuation) at 60 GHz is much more severe than the path loss at the frequencies that are currently employed for Wireless Personal Area Networks (WPAN). Theoretical description for this phenomenon is provided by Friis formula [9], according to which attenuation in the air is proportional to the frequency squared. It is known that the line-of-sight (LOS) attenuation of the 60 GHz wireless channel can be modeled with a log-normal model [11]. Parameters for this model have been defined through the extensive measurements presented in a number of publications. Summary on the parameters for different experimental environments can be found in [9]. We perform the modeling of the system without taking into account frequency dependency of the path loss. To the best of our knowledge, frequency dependent models for 60 GHz system have not yet been reported.

Influence of the noise on the signal can be modeled with the following formula [10,11]:

$$SNR = P_{tx} + G_T + G_R + G_{LNA_{tx}+PA_{tx}} + G_{LNA_{rx}+PA_{rx}} - PL -$$
$$-(10 \log_{10}(KTB) + NF_{LNA_{tx}+PA_{tx}} + NF_{LNA_{rx}+PA_{rx}}),$$ (3)

$$PL = PL(d_0) + 10n \log_{10}(\frac{d}{d_0}),$$ (4)

where P_{tx} in our case is the RF power on the output of the PD, G_T and G_R are the gain of transmitting and receiving antennas respectively, $G_{LNA_{tx}+PA_{tx}}$ and $G_{LNA_{rx}+PA_{rx}}$ are gains of

amplification cascades at transmitting and receiving parts of the scheme respectively, PL is the distance-dependent path loss (attenuation) in the air. The terms in brackets represent noise contributions. The first term represents the Johnson noise, second and third represents noise contributions from amplifiers. Parameters d_0 and d in Eq. (4) represent the reference distance (we used 1 m according to [9]) and the distance between a transmitter and a receiver respectively, n denotes path loss exponent.

The formula does not account for shadowing caused by LOS obstruction, but this resembles the experimental setting where we were working with the LOS scenario only.

Phase noise modeling for the channel was excluded after the experimental examination of the phase noise of the oscillator presented in Fig. 3. Figure 3 shows the high quality of the electrical oscillator for 3 cases: measuring the phase noise of LO, setup without fiber transmission up to a transmitting antenna (optical back-to-back) and after 20 km of NZDSF. Figure 3 also illustrates the fact that contribution from the system to the phase noise is insignificant. Moreover, it could be excluded from consideration, because after wireless transmission we finally recover with ED only the amplitude of the signal, and therefore discard information about phase or frequency.
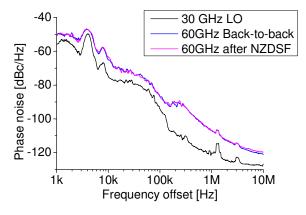

Fig. 3. Phase noise of RF subcarriers.

The model does not take into account the nonlinear effects that are reported for Power Amplifiers in [9]. Nevertheless we regard the model as feasible since the power after the PD is low, so we work in the linear region. Indeed, the power on the output of the PA at the transmitting side given the power at the photodiode of −10 dBm is around −6 dBm. Typically nonlinear effects are observed in the region above 0 dBm [9]. The RF-spectrum measured is depicted in Fig. 4. We refer to the power before the antenna, as the power before radiation P_{br}. Therefore the equation for wireless channel simulation based on Eq. (3) and Eq. (4) could be transformed into:

$$SNR = P_{br} + G_T + G_R + G_{LNA_{rx}+PA_{rx}} - PL(d_0) - 10n\log_{10}(\frac{d}{d_0}) - $$

$$-(10\log_{10}(KTB) + NF_{LNA_{tx}+PA_{tx}} + NF_{LNA_{rx}+PA_{rx}}). \tag{5}$$
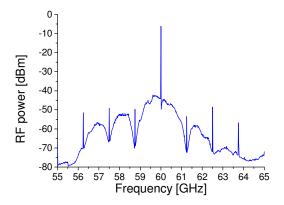
Fig. 4. RF spectrum measured before the antenna.

Typical parameters for the path loss at the reference distance and the path-loss exponent has been found in the references [9,10]. Values for the parameters that are used in modeling of the wireless channel are listed in the Table 1 below.

Table 1. System Parameters for Modeling

Parameter	Numerical value
Center frequency, GHz	60
Joint noise figure Tx amplifiers (LNA + PA), dB	(6 + 7) = 13
Joint noise figure Rx amplifiers (LNA + PA), dB	(6 + 7) = 13
Joint gain of Tx amplifiers (PA + LNA), dB	(28.7 + 16) = 44.7
Joint gain of Rx amplifiers (PA + LNA), dB	(28.7 + 16) = 44.7
Gain of the Tx antenna, dBi	20
Gain of the Rx antenna, dBi	20
Bit rate, Mbps	312.5/1250
Distance, m	2-6
Reference path loss at 1 meter, dB	57.5
Path loss exponent	1.77
Ambient temperature for Johnson noise modeling, K	298

We perform attenuation of the signal and addition of the Additive White Gaussian Noise (AWGN) in VPI, the noise power and attenuation to achieve SNR described in Eq. (5) are calculated in Matlab.

4. Results and discussion

Our goal for optimization is to achieve the best video delivery quality for a given link budget. With regards to the role of the quantization of transform coefficients of the coded video in the optimization, roughly speaking, the smaller the quantization parameter size, the smaller the source distortion (loss due to compression), but the larger the channel distortion it may cause. In the experiment we explored two cases. First, the chosen test video sequence ('blue sky' 4:4:4) was encoded with bitrate of 312.5 Mbps. Second, the tested video sequence was encoded in a high quality setting with the quantization parameter equal to 1, which gave us a compression ratio of 3.
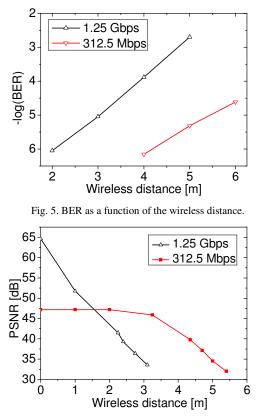
Fig. 5. BER as a function of the wireless distance.

Fig. 6. PSNR as a function of the wireless distance.

On the Fig. 5 BER at the power level at the photodiode equal to −10 dBm as a function of the wireless distance is depicted. From the Fig. 5 we can see that in general the distortion induced by the wireless channel is severe in our system, but video coded with the use of higher quantization parameter has greater dynamic range of wireless distance, as shown in Fig. 6. The distance equal to 0 corresponds to the distortion introduced by the compression only. When we increase the wireless distance, in the beginning, the source distortion is dominant, and the use of lower quantization parameter is reasonable. Anyhow, we lose the advantage of lower distortion after around 2 m of transmission when video is evaluated based on the PSNR metric only. This shows the potential of optimization of the power budget of the system under the constraint of video quality. We obtain similar curves for changing optical power level at the photodiode at 5 m of wireless distance, as shown in Fig. 7 and Fig. 8. With the higher video compression we can work at lower optical power levels. At the same time, we should note that the video quality is high in both cases, and deterioration induced by the compression itself can be regarded as non-significant (PSNR of the video unimpaired by the channel is higher than 45 dB in both cases).
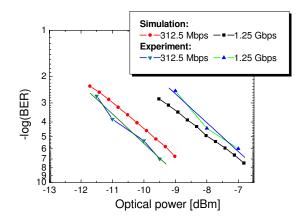
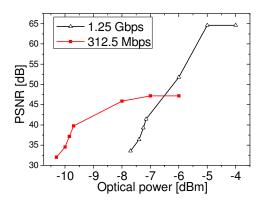Fig. 7. BER as a function of the optical power at the photodiode.

Fig. 8. PSNR as a function of the optical power at the photodiode.

Curves provided by simulation for 5 meters distance and dynamically changing optical power levels show close resemblance that verifies the correctness of the simplified wireless channel model employed. We do not provide simulation-based curves for PSNR, because our simulation is based on the analytical estimation of BERs with the use of VPI software, and we therefore do not have traces including erroneous bits to analyze video performance.

5. Video coding for 60 GHz radio-over-fiber

We employed video coding parameters in a simplified setting that is suitable for both conferencing applications and distributed video gaming. The main constraints for such type of an application are delay and energy consumption. As a part of simplified setting we were using Universal Variable Length Coding (UVLC) for entropy coding that is considered a lower complexity solution [7]. All coding experiments were performed in intra mode thus eliminating the need for long buffering time, and satisfying low delay requirement. The simulation below was performed with bit traces including erroneous bits.

H.264/AVC encoder employs the number of error-resilience tools: slicing of the frame, data partitioning, arbitrary slice ordering, and redundant coded slices [7]. Below we present simulation on two major tools providing error resilience: slices and Flexible Macroblock Ordering (FMO). On the decoder side, there are two error concealment tools used in JM 17.0 reference software implementation of H.264/AVC codec, one exploiting spatial information only, suitable for intra frames (the one used in the experiment and simulation), and one

exploiting temporal information. Details on the error concealment algorithms used can be found in [5].

First we performed the simulation with a different size of the packet (each containing one slice of the frame). Employing the smaller slices enables us to receive acceptable video quality in the regions with higher BER, and therefore extends distance for acceptable quality of video transmission. Indeed, enabling packets of shorter length reduces the amount of information lost when the packet is discarded, enabling decoder to reconstruct impaired parts of the picture better from unimpaired blocks of neighboring pixels. The simulation results are illustrated on Fig. 9.
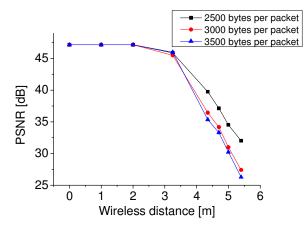

Fig. 9. PSNR as a function of the wireless distance for different packet sizes of the encoded video for the bitrate of 312.5 Mbps.

Below we also present the simulation results for enabling FMO in H.264 reference software [5]. H.264/AVC is the first standard defining this error-resilience tool [7]. In case if we do not use FMO, the images will be composed of a single slice groups with the macroblocks in a scan order. If we employ this algorithm, then when we lose a slice of the video frame, we can make better approximation with the neighboring blocks and therefore, presumably, can achieve gain in PSNR. Results of the simulation for the packet size of 3000 bytes are depicted in the Fig. 10. FMO shows up to 3 dB improvement of PSNR.
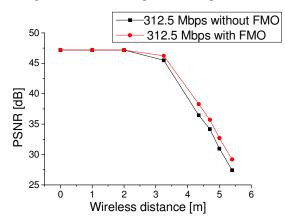

Fig. 10. PSNR performance as a function of the wireless distance for FMO effect estimation.

Coding simulations show the effect of employed source coding error-resilience mechanisms for a particular simplified setting of H.264/AVC and 60 GHz RoF setup as an example of physical layer architecture suitable for transmission high quality HD video

content. Employed tools of H.264/AVC show the greater robustness of video provided by advanced video coding against impairments induced by 60 GHz fiber-wireless channel.

6. Conclusions

Our experiment and simulation demonstrates the trade-off between the distortion introduced by the source (lossy compression) and distortion introduced by channel for high quality HD video transmission over 60 GHz RoF fiber-wireless links. We have achieved significant extension of wireless distance employing low complexity physical layer solution for detection of RF modulated signal. Our work demonstrates the solutions for improving robustness and reach of simplified converged fiber-wireless RoF communication links provided by advanced video coding.

Acknowledgments